Evolution from tunneling to hopping mediated triplet energy transfer from quantum dots to molecules

Zhiyuan Huang,[$,a] Zihao Xu,[$,b] Tingting Huang,[a] Victor Gray,[c,d] Kasper Moth-Poulsen,[c] Tianquan Lian,[b*] Ming Lee Tang[a*]

[a] Department of Chemistry, University of California, Riverside, Riverside, CA, 92521, United States

[b] Department of Chemistry, Emory University, Atlanta, GA, 30322, United States

[c] Department of Chemistry and Chemical Engineering, Chalmers University of Technology, 412 96 Gothenburg, Sweden

[d] Department of Chemistry – Ångström Laboratory, Uppsala University, Box 523, 751 20 Uppsala, Sweden.

[$] Authors contributed equally

Abstract

Efficient energy transfer is particularly important for multi-excitonic processes like singlet fission and photon upconversion. Observation of the transition from short-range tunneling to long-range hopping during triplet exciton transfer from CdSe nanocrystals to anthracene is reported here. This is firmly supported by steady-state photon upconversion measurements, a direct proxy for the efficiency of triplet energy transfer (TET), as well as transient absorption measurements. When phenylene bridges are initially inserted between a CdSe nanocrystal donor and anthracene acceptor, the rate of TET decreases exponentially, commensurate with a decrease in the photon upconversion quantum efficiency from 11.6% to 4.51% to 0.284%, as expected from a tunneling mechanism. However, as the rigid bridge is increased in length to 4 and 5 phenylene units, photon upconversion QYs increase again to 0.468% and 0.413%, 1.5–1.6 fold higher than that with 3

phenylene units (using the convention where the maximum upconversion quantum efficiency is 100%). This suggests a transition from exciton tunneling to hopping, resulting in relatively efficient and distance-independent TET beyond the traditional 1 nm Dexter distance. Transient absorption spectroscopy is used to confirm triplet energy transfer from CdSe to transmitter, and the formation of a bridge triplet state as an intermediate for the hopping mechanism. This first ~~demonstration of long-range energy transfer~~ observation of the tunneling-to-hopping transition for long range triplet energy transfer between nanocrystal light absorbers and molecular acceptors suggests that these hybrid materials should further be explored in the context of artificial photosynthesis.

Introduction

Efficient long-distance energy transfer in artificial photosynthetic platforms is a long-standing goal. It is currently understood to occur via incoherent hopping or adiabatic energy transfer.[1-3] Compared to exciton transport, charge transfer is significantly better understood. Solid-state semiconductor devices and individual cytochrome proteins rely on single short (<1 nm) and long-range (2.5 nm) electron tunneling steps, respectively[4-7]. Charge transfer between component cytochromes in the photosynthetic reaction centers requires multi-step tunneling or incoherent electron hopping[5, 8-9]; polycrystalline organic semiconductor thin films generally rely on both hole and electron hopping[10]. In contrast, exciton transport requires the correlated transfer of both the electron and the hole[11-12]. Rates of energy transfer have to be deconvoluted into hole and electron contributions, and identification of the possible pathways involved is key to achieving efficient energy transfer, especially for soft materials like proteins, organic materials, and colloidal nanoparticles.

Colloidal semiconductor nanocrystals (NCs) are promising materials in optoelectronic applications such as photovoltaics, light emitting diodes and photodetectors, etc.[13-18] Rapid energy and charge transport over long distances is one of the prerequisites for high performance devices. Many studies have shown photoexcited nanocrystals can efficiently transfer charge directly to surface bound molecules,[19] or across inorganic shells,[20] but much fewer studies have been performed on triplet energy transfer from NC photosensitizers. In terms of exciton transport, long-lived triplet excitons, with diffusion lengths up to several micrometers in crystalline organic solids,[21-22] are promising for long-distance energy transfer. In comparison, the short diffusion length of singlet excitons (tens of nanometers) limits the thickness of organic photovoltaic devices to ~100 nm and precludes the complete absorption of sunlight.[23] Though well studied in organic donor-bridge-acceptor (D-B-A) systems,[24-27] long-range triplet exciton transport relating to semiconductor NCs has not been reported so far. Precedence lies in mechanistic charge transfer studies in labelled cytochrome proteins, and in molecular D-B-A systems. Despite the heterogenous nature of proteins, single step electron tunneling up to 2.6 nm has been experimentally measured with an exponential distance constant, β ~11 nm^{-1}.[1, 9] Short conjugated bridges in organic donor-acceptor systems retain this exponential distance-dependent tunneling for electron transfer but report smaller β values[6]. We showed previously that[28] triplet energy transfer from CdSe NCs to anthracene displays this exponential distance dependence with varying lengths of phenylene bridges. However, longer bridges show an ohmic distance-dependent hopping mechanism.[29] Weak distance dependence has also been ascribed theoretically to adiabatic electron transfer[2-3]. Optimization of the structure and energetics of the donor, bridge, and acceptor to accentuate charge hopping and avoid the strong distance-dependent charge tunneling processes are crucial for realizing wire-like long-range charge transport.

In this work, we demonstrate the transfer of triplet excitons from semiconductor NCs to molecular acceptor can occur via tunneling or hopping, and the mechanism is controlled by the triplet energy level of the intervening *p*-oligophenylene bridge. With CdSe NCs as triplet energy donors, anthracene acceptors attached by a pyridine anchoring group and *p*-oligophenylene bridge, we show that the triplet energy transfer mechanism changes from tunneling (with an exponential distance dependence) to hopping. The tunneling-to-hopping transition was observed from steady-state photon upconversion quantum efficiency (QY) measurements. The shortest three ligands show the expected distance dependent decrease with increasing bridge length, while the last two ligands with the longest bridge show an unexpectedly high upconversion QY with no distance dependence. Transient absorption spectroscopy supports this interpretation with the observation of both the triplet state of the anthracene acceptor, and the phenylene bridge. This work shows that molecular design is critical in enabling the first demonstration of long-range triplet exciton transport between semiconductor NCs and organic acceptors.

Results and discussion

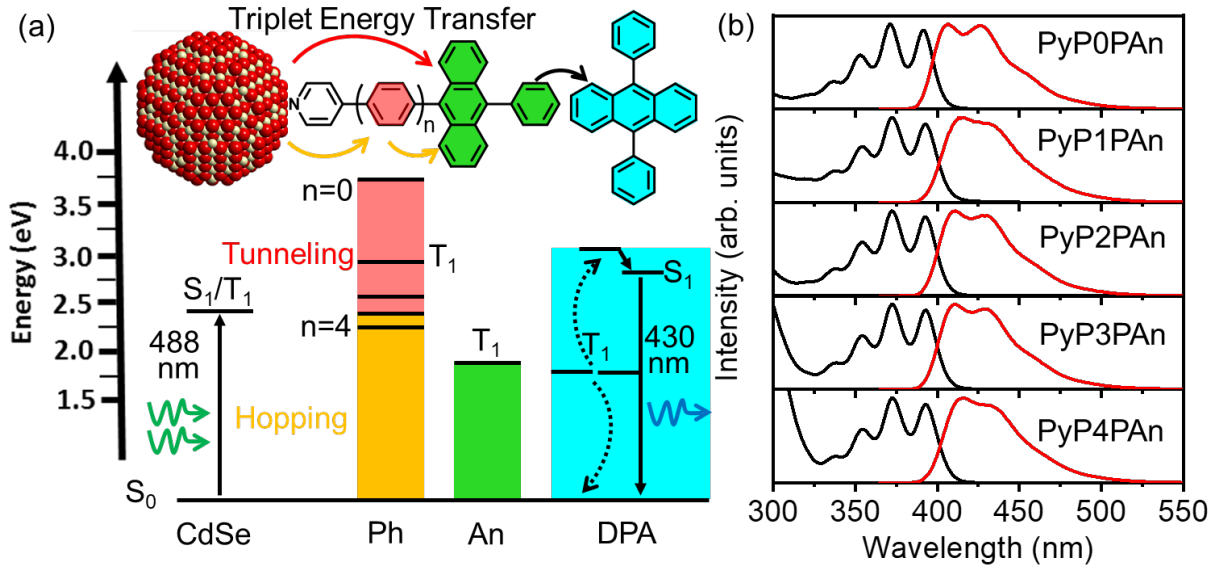

Figure 1. (a) Illustration of energy diagram of energy transfer process involved in CdSe NC sensitized photon upconversion. Red arrows denote triplet exciton tunneling while orange yellow arrows denote hopping. (b) Absorption (black) and fluorescence (red) spectra of transmitter ligands with different length of phenylene bridges. The spectra were obtained with hexane at room temperature.

The mechanism of CdSe nanocrystal (NC) sensitized photon upconversion is presented in Figure 1. This three-component upconversion platform comprises of 2.4 nm diameter CdSe NCs as the light absorber, anthracene with a phenylene bridge and pyridine binding group as the transmitter, and 9,10-diphenylanthracene (DPA) as the emitter. Photon upconversion is initiated by photoexcitation of CdSe NCs with a 488 nm continuous wave laser. After intersystem crossing within CdSe NCs, the triplet exciton is transferred to the surface anchored anthracene by tunneling or hopping through the phenylene bridge. Subsequent TET occurs from the transmitter to the emitter DPA. Two DPA triplets then annihilate to form a singlet, followed by the fluorescence of DPA at 430 nm (Figure S1). In this hybrid upconversion system, each component is rationally

designed. As upconversion QYs negatively correlate with the NC size,[30-31] small CdSe NCs are used, resulting in high upconversion quantum yields. Furthermore, without the transmitters in Scheme 1, the native oleate ligand shell hinders energy transfer from CdSe NCs to DPA, leading to a low upconversion QY. The transmitter ligands funnel the triplet energy from CdSe NCs to DPA and have been reported to enhance upconversion (QYs) as much as 3 orders of magnitude.[32] Lastly, DPA is selected as the light emitter due to its high fluorescence QY (90%).[33]

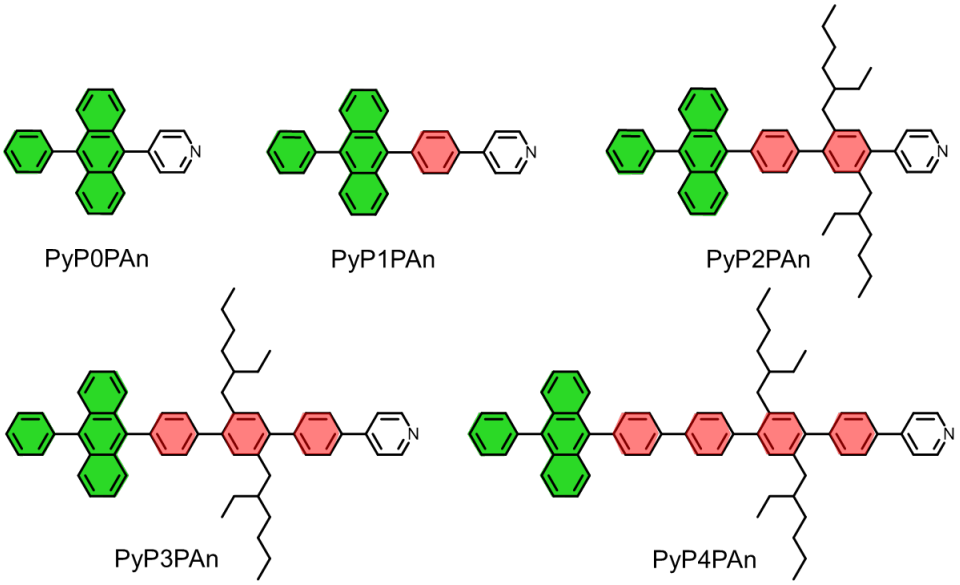

Scheme 1. The structures of transmitter ligands with different length of phenylene bridges.

The transmitter ligands are designed with different lengths of phenylene units to vary the bridge triplet energies between CdSe and anthracene. The structures of the 5 transmitters are presented in Scheme 1. The 9-phenylanthracene core possesses an excited triplet state, T_1, with the energy similar to that of DPA (1.77 eV),[34-35] and lower than that of CdSe (2.47 eV). Pyridine serves as the anchoring group binding anthracene to the surface of CdSe NCs, and the phenylene bridges as the rigid spacer to control the distance between CdSe NCs and anthracene. As transmitter ligands are loaded on CdSe NCs by a solution-based ligand exchange reaction (see SI), ethylhexyl

side chains are incorporated on PyP2PAn, PyP3PAn and PyP4PAn to maintain solubility. As shown in Table 1, all transmitters possess high fluorescence QYs (> 65%), meaning reduced nonradiative decay. These ethylhexyl side chains introduce steric bulk and rigidity and may explain the higher fluorescence QY of PyP2PAn (79.6%) compared to PyP1PAn (74.1%). The absorption and fluorescence spectra of transmitters are shown in Figure 1b and S3. From these spectra, we can see that while the presence of the phenylene bridges does not modify the singlet electronic states of anthracene core (also confirmed by TA spectra and kinetics in Figure S5-S6), growth in the number of phenylene units increases the absorption at 300 nm from PyP0PAn to PyP4PAn. As the number of phenylene units, **n**, increases from 0 to 4, the corresponding lowest excited triplet state, T_1, of this bridge decreases from 3.68 eV for pyridine[36], 2.84 eV for biphenyl, 2.53 eV for *p*-terphenyl[35, 37] to 2.37 and 2.34 eV[26, 38] respectively for the two longest transmitters (Figure 1a). With this design, the triplet exciton is expected to transfer from CdSe NCs to the anthracene core by superexchange through the phenylene bridge when the bridge's T_1 energy exceeds the bandedge exciton of CdSe NCs (n=0, 1, 2). On the other hand, when n=3 or 4 (PyP3PAn and PyP4PAn), the bridge's T_1 state can be thermally populated, which allows triplet exciton transport from CdSe NCs to anthracene by hopping mechanism with a weak distance dependence. ~~and a weak distance dependence is expected, either through hopping or adiabatic energy transfer. Close examination of the vibrational fine structure in the absorption spectra (Fig. S3) shows a red shift in the anthracene core on the two transmitter ligands with the shortest bridges when bound on the surface of CdSe NCs (compared to the free ligands in solution). This is accompanied by a slight red shift in the NC PL for CdSe/PyP0PAn and CdSe/PyP1PAn (Fig. S4). These bathochromic shifts in both anthracene absorption and NC bandedge PL could be due to the~~

~~delocalization of CdSe exciton to anthracene for the two shortest ligands, not observed for the last three ligands with longer phenylene bridges.~~

Table 1. Key parameters of pyridine transmitter ligands. Φ_{FLT}, the fluorescence quantum yield; C_{opt}, the optimal concentration of transmitters during ligand exchange; Φ_{UC}, upconversion quantum efficiency; Φ_{TET}, the efficiency and, k_{TET}, the rate constant of triplet energy transfer from CdSe nanocrystal to transmitters.

Ligand	Bridge T_1 (eV)	Φ_{FLT} (%)	C_{opt} (mM)	Φ_{UC} (%)[a]	Φ_{TET} (%)[b]	k_{TET} (μs^{-1})[c]
PyP0PAn	3.68	90.2	21.7	11.6	30.1	54.0
PyP1PAn	2.84	74.1	7.85	4.51	11.7	2.68
PyP2PAn	2.53	79.6	1.70	0.284	0.737	0.139
PyP3PAn	2.37	79.1	2.55	0.468	1.21	0.229
PyP4PAn	2.34	68.6	5.37	0.413	1.07	0.202

[a] Φ_{UC} of 100% is defined as the emission of one high energy photon per two absorbed low energy photons. [b] CdSe/PyP0PAn Φ_{TET} is measured by TR-PL and calculated as shown in SI section 9 and Table S2. For CdSe/PyP1PAn to CdSe/PyP4PAn, Φ_{TET} is calculated from Φ_{UC} assuming all other efficiencies are the same according to Eq.1. [c] Similarly, k_{TET} is measured by TR-PL for CdSe/PyP0PAn. For CdSe/PyP1PAn to CdSe/PyP4PAn k_{TET} is calculated by Eq. 2.

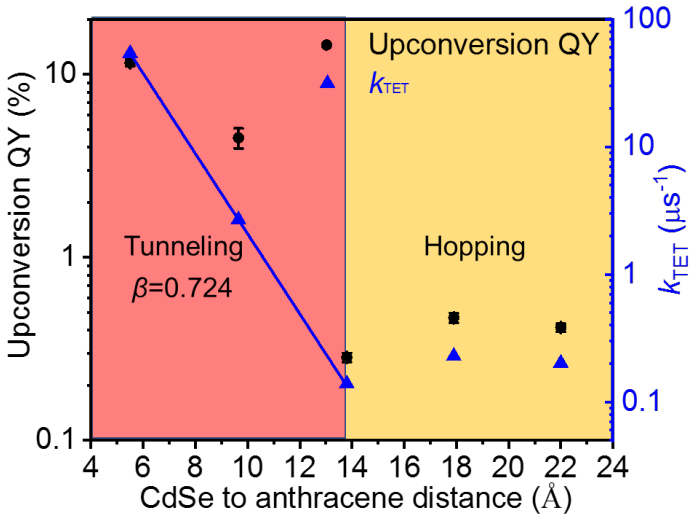

Figure 2. Dependence of upconversion quantum efficiencies and triplet energy transfer rate constants on the length of phenylene bridges. The solid blue line is the linear fit of the k_{TET} for the first three data points, with the slope (damping coefficient) of 0.7236±0.0005 $Å^{-1}$.

The upconversion quantum efficiencies of this three-component system were measured as a function of the transmitter spacer length. Upconversion QYs are optimized by varying the surface loading of transmitters (see SI, Figure S2) and the optimal upconversion QYs are listed in Table 1. In Figure 2, the optimal upconversion QYs are plotted as a function of the distance between the CdSe NC donor and anthracene acceptor, defined as the distance from the ligand binding site (nitrogen in pyridine) to the center of anthracene. The upconversion QY for the shortest transmitter (PyP0PAn) is 11.6%. This is an increase by two orders of magnitude compared with the free CdSe NCs with no transmitters (0.1%). As the phenylene bridge units in the transmitter ligands increase, the upconversion QYs drop exponentially to 4.51% for PyP1PAn and 0.284% for PyP2PAn. To our surprise, the upconversion QYs of PyP3PAn and PyP4PAn (n=3 and 4) increase compared to the shorter PyP2PAn (n=2) ligand and become weakly dependent on spacer length. This result

suggests that the mechanism of exciton transfer changes from exciton tunneling at n<3 to hopping or adiabatic energy transfer at n>3. Although the upconversion efficiency depends on the efficiencies of multiple steps, we will show below that in these systems with different transmitters, the TET rate from the NC to transmitter (k_{TET}) is the key parameter that is different while other parameters remain nearly constant. As a result, the observed distance dependence in the upconversion efficiency reflects that distance dependence of k_{TET}. Similar distance dependence was observed in previously reported triplet energy transfer rates [25-28, 39] and charge transfer rates[40-41] through related molecular bridges.

The upconversion QY ($\emptyset_{UC}$) depends on the product of the quantum efficiencies of TET from CdSe NCs to transmitters($\emptyset_{TET}$), triplet-triplet annihilation of emitters ($\emptyset_{TTA}$) and emitter fluorescence ($\emptyset_{FL}$), as shown in Eq (1):

$$\emptyset_{UC} = \emptyset_{TET} \cdot \emptyset_{TTA} \cdot \emptyset_{FL} \quad (1)$$

We have assumed that the quantum efficiency of triplet energy transfer from the transmitter to the emitter is nearly 100% for all transmitters, independent of spacer length. The validity of such assumption will be further discussed below with the help of transient absorption studies. $\emptyset_{TTA}$ and $\emptyset_{FL}$ depend only on the emitter, which are kept identical in these measurements. Thus, the transmitter dependent upconversion efficiency reflects the distance dependence of $\emptyset_{TET}$. $\emptyset_{TET}$ is determined by the relative rates of triplet energy transfer (k_{TET}) and the intrinsic decays of the NC, according to Eq. (2):

$$\emptyset_{TET} = \sum_{i=1}^{3} \frac{a_i k_{TET}}{k_{TET} + k_{CdSe,i}} \quad (2)$$

In Eq. (2) $k_{CdSe,i}$, and a_i are the rate constant and amplitude of the ith component of the multi-exponential intrinsic decay of CdSe NCs obtained from TR-PL as shown in Table S2. In the limit

that k_{TET} is small compared to k_{CdSe}, Eq. 2 can be approximated to $\emptyset_{TET} = k_{TET}/k_{CdSe}$, which means that $\emptyset_{TET}$ depends linearly on k_{TET}, and by Eq. 1 $\emptyset_{UC}$ also depends linearly on k_{TET}.

In the following kinetics study, the samples are prepared with the same QD and mediator loading as in the upconversion measurement, the only difference is that DPA (annihilator), which absorbs strongly in the QD emission and mediator absorption regions, have been removed to allow time-resolved photoluminescence (PL) and transient absorption (TA) studies of the TET process between the QD and mediator. In CdSe/PyP0PAn sample, the NC PL decay is significantly faster than in pristine CdSe samples (Figure S7a), from which k_{TET} can be determined to be 54.0 μs^{-1}. Using Eq. 2, $\emptyset_{TET}$ can be determined to be 30.1%, as shown in Table 1. From the measured $\emptyset_{UC}$(11.6%) and $\emptyset_{TET}$ and reported DPA $\emptyset_{FL}$ =90%,[33] $\emptyset_{TTA}$ can be calculated to be 42.8% according to Eq. 1. This corresponds well to $\emptyset_{TTA}$ values reported in literature[42-43]. However, for emitters with longer spacer lengths (n=1-4), k_{TET} becomes much slower than the intrinsic decay of NCs, and it is difficult to extract a contribution from TET by comparing the total decay rates in NC/transmitter complexes ($k_{CdSe}+k_{TET} \approx k_{CdSe}$) with the decay rate of free NCs (k_{CdSe}), as shown in Figure S7b. Alternatively, for CdSe/PyP1PAn to CdSe/PyP4PAn, the $\emptyset_{TET}$ can be calculated from measured $\emptyset_{UC}$ according to Eq. 1 using $\emptyset_{TTA}$ and $\emptyset_{FL}$ determined above. Then the rate constant of TET from CdSe NCs to anthracene (k_{TET}) can be calculated from Eq. 2. The results are listed in Table 1 and plotted in Figure 2.

For Dexter energy transfer, k_{TET} decays exponentially with an increase in distance between donor and acceptor, following Eq. (3):[44-45]

$$k_{TET} = k_0 \cdot e^{-\beta d} \qquad (3)$$

where k_0 is the pre-factor and β is the damping coefficient that describes the exponential decay of the electronic coupling between CdSe NCs and anthracene. Here, the effective transfer rate is calculated and plotted in Figure 2. The effective transfer rate is the product of TET rate for a single transmitter and the total number of transmitters per CdSe NC. In this study, due to the relatively weak binding of the pyridine group, the binding of the transmitter to CdSe NC is reversible, which means there is a population distribution between the bound and free transmitter. This is confirmed by the observation of ligand detachment on UV-Vis absorption spectra after washing CdSe/PyP0PAn complex a second time (Figure S2f). Therefore, the exact number of bound transmitters per NC is difficult to determine. However, it's been shown in previous work that an optimal number of bound transmitters exists, because transmitter triplets can annihilate at high surface density which is detrimental to upconversion QYs.[46-47] Therefore, the optimal number of transmitters should be as high as possible to maximize the TET efficiency, but not surpass the loading that could initiate triplet-triplet annihilation of transmitters. Considering the similar structure of anthracene core for different transmitters, i.e. similar threshold surface density that transmitter triplet-triplet annihilation occurs, we assume the number of bound transmitters with optimal upconversion QYs would be similar, and the effective rate is used in Figure 2 to represent the dependence of rate on distance. Fitting the k_{TET} of PyP0PAn, PyP1PAn, and PyP2PAn yields an exponential distance dependence, as shown in Figure 2, with a damping coefficient of 0.724 $Å^{-1}$. This value is comparable with previously reported values for triplet[24, 26-28] or charge transfer[40-41] in D-B-A systems with the *p*-oligophenylene bridge, considering the damping coefficient of triplet transfer is the sum of that for electron and hole transfer.[48-49] This superexchange mechanism is expected because of the electronic coupling between the CdSe donor and anthracene acceptor is approximately exponentially dependent.

The TET rate constants of PyP3PAn and PyP4PAn (n=3 and 4) increase compared with the shorter PyP2PAn (n=2) ligand, as shown in Figure 2. As the length of phenylene bridge increases, the extended conjugation decreases the energy of T_1 state of phenylene bridge, bringing it near resonance with the donor state (Figure 1a). The triplet exciton then transfers by incoherent hopping through the T_1 state of the phenylene bridge instead of tunneling, which gives rise to the weak distance dependence observed for PyP3PAn and PyP4PAn. Alternatively, a weak distance dependence can also occur in the adiabatic energy transfer limit with strong electronic coupling between CdSe NC donor and molecular acceptor. Close examination of the vibrational fine structure in the absorption spectra (Fig. S3) shows a red shift in the anthracene core on PyP0PAn and PyP1PAn when bound on the surface of CdSe NCs (compared to the free ligands in solution). This is accompanied by a slight red shift in the NC PL for CdSe/PyP0PAn and CdSe/PyP1PAn (Fig. S4). These shifts in both anthracene absorption and NC bandedge PL could be due to the delocalization of CdSe exciton to anthracene for the two shortest ligands, ~~redshift is observed in both ligand absorption and CdSe NC PL spectra due to the binding of PyP0PAn and PyP1PAn to CdSe NC surfaces (Figure S3a, b and Figure S4b),~~ indicating a strong CdSe-transmitter coupling. However, no change is observed for CdSe/PyP2PAn-CdSe/PyP4PAn complexes, suggesting weak coupling between NC and ligands (Figure S3, S4). Strong electronic coupling between CdSe, the bridge and anthracene is prevented by the 30-35º torsional angle between the last phenyl unit and anthracene[40, 50]. Therefore, the weak distance dependence for PyP3PAn and PyP4PAn is ascribed to incoherent hopping. Further support of this pathway is the presence of the bridge triplet state as the intermediate between the triplet states of the donor and acceptor, which is directly observed in transient absorption spectroscopy to be discussed below.

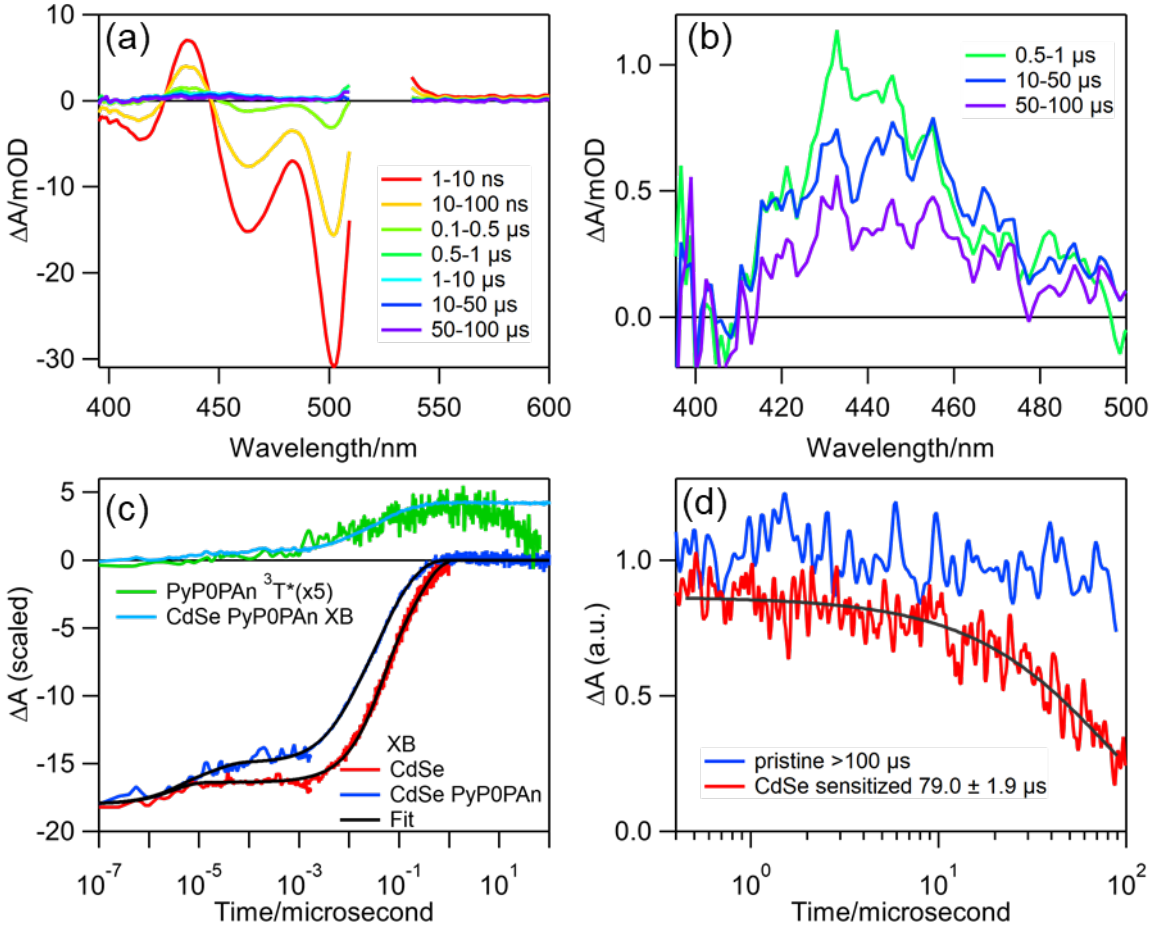

Figure 3. (a) Nanosecond transient absorption of CdSe/PyP0PAn. The sample was pumped at 510 nm to avoid direct excitation of PyP0PAn. The 510 nm region is not shown due to pump scattering. (b) The excited state absorption of PyP0PAn triplet state at the 400-500 nm region. (c) The comparison of CdSe exciton bleach probed at 500 nm with (blue) and without (red) surface bound PyP0PAn, and the corresponding PyP0PAn triplet kinetics probed at 446 nm (green), which is an isosbestic point for the CdSe QD transient spectra. The CdSe\PyP0PAn XB is scaled (light blue) and compared with the triplet kinetics. (d) Comparison of the triplet lifetime of pristine PyP0PAn and CdSe sensitized probed at 440 nm. No obvious decay observed for pristine PyP0PAn in this 100 microseconds time window. The CdSe sensitized triplet is fitted to a single exponential decay $e^{-t/\tau}$.

Transient absorption (TA) spectroscopy is used to confirm triplet exciton transfer from CdSe NCs to transmitters. Samples of CdSe NCs capped with transmitter ligands with optimal ligand loadings are prepared for TA measurements (without DPA). Figure 3a shows the TA spectra of CdSe/PyP0PAn measured with 510 nm excitation at an excitation energy density of 200 $\mu J/cm^2$, which selectively excites CdSe QDs. The positive features represent the excited state absorption (ESA), and the negative features the ground state bleach (GSB). The ESA of the T_1 state of anthracene lies around 440 nm, overlapping with the ESA of CdSe NCs. After 500 ns, when the CdSe ESA has decayed completely, the T_1-T_n transition of PyP0PAn peaked at 440 nm can be clearly observed (Figure 3b). The kinetics of triplet growth can be obtained at 446nm, at which the CdSe QD has negligible contribution to the TA signal (Figure 3c). Compared with free CdSe QDs, the exciton bleach (XB) kinetics of CdSe/PyP0PAn show a faster recovery (Figure 3c), consistent with exciton quenching by TET from the QD to PyP0PAn. The QD XB bleach and PyP0Pan triplet growth shows good agreement with each other, with the exception of early delay times (< 1 ns), during which there is noticeable decay of QD XB signal without the corresponding growth of PyP0Pan triplet. We attribute this to surface electron traps caused by the ligand exchange process used for attaching the transmitter molecules.[51] The kinetics of exciton bleach probed at 500 nm with/without mediator was fit to extract the rate of TET and the fitting parameters are listed in SI Table S2. The TET rate is determined to be 31.5 μs^{-1}, and from which the triplet yield is determined to be ~60% (see SI Section 9 for details). Both values are comparable to those determined from PL quenching (k_{TET} ~54 μs^{-1}, and $\emptyset_{TET}$~30%) and shown in Table 1. Unfortunately, as shown in Figure 3b, the triplet absorption signal in CdSe/PyP0PAn, the complex with the highest $\emptyset_{TET}$, is already small (~1 mOD). Similar TA studies conducted on the transmitter

ligands with longer phenylene bridges (n=1, 2, 3 and 4) become difficult due to much lower $\emptyset_{TET}$ and smaller triplet signal. Furthermore, due to the slower TET rate, and the exciton bleach kinetics shows negligible difference with/without the transmitter (Figure S7d). Therefore, the rate and efficiency of TET is only measured by time-resolved spectroscopy for the shortest ligand, PyP0PAn, by both TA spectra and time-resolved photoluminescence (Figure S7). For all other ligands, these values are calculated from steady-state $\emptyset_{UC}$ measurements.

The fit of the triplet decay kinetics shown in Figure 3d also reveals that the triplet lifetime of PyP0PAn is shortened from over 100 μs in solution to ~80 μs when grafted on CdSe NC surface (Figure 3d and S4). With such a long triplet life time and high DPA concentration (2.15 mM) in this upconversion system, the TET efficiency from transmitters to DPA can be estimated based on $\Phi_{TET2} = \frac{k_{TET2}[DPA]}{k_{TET2}[DPA]+k_T}$, where k_{TET2} is the bimolecular TET rate constant between transmitter and DPA (~30 $\mu s^{-1}M^{-1}$ based on a previous study[52]), and k_T is the transmitter triplet lifetime (80 μs, equivalent to 0.0125 μs^{-1}). The calculated TET efficiency from NC-surface bound transmitters to DPA is estimated to be over 84%. In our analysis, it is approximated to be unity and constant for all transmitters.[53]

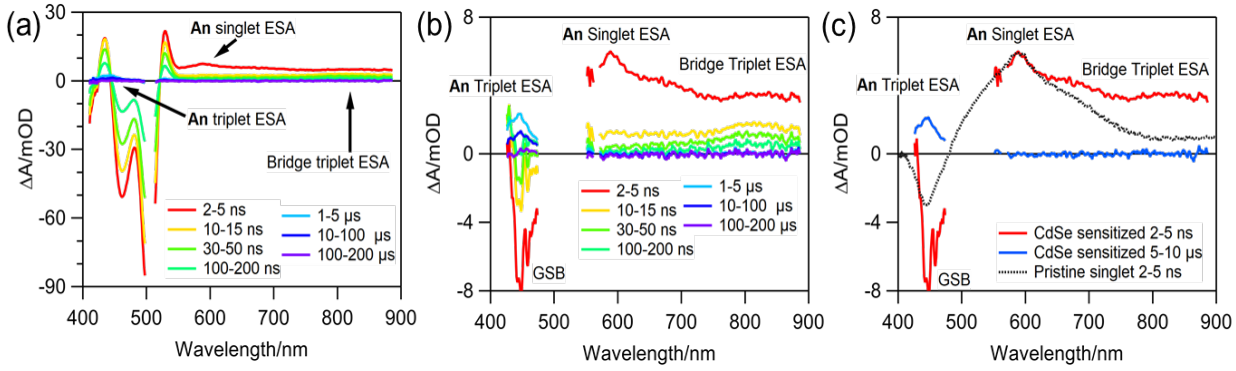

Figure 4. TA absorption spectra of CdSe/PyP4PAn. (a) Nanosecond transient absorption of CdSe/PyP4PAn measured with 510 nm excitation. Sample: 4.06 μM CdSe NCs and 0.182 M PyP4PAn dissolved in THF with no DPA (annihilator). (b) TA spectra in panel a) after subtraction of CdSe contribution. (c) Comparison of subtracted TA spectra of CdSe/PyP4PAn (from panel b) at 2-5 ns (red) and 5-10 μs (blue) with the TA spectrum of pristine PyP4PAn at 2-5 ns (grey line). The spectra for pristine PyP4PAn were measured with 400 nm and the full spectra at other delay times are shown in Figure S5.

Although challenging to measure the rate of TET in longer transmitter ligands, TA spectroscopy is able to observe the triplet excited state in the bridge of PyP4PAn as an intermediate state between the recovery of the CdSe NC exciton bleach and rise of the triplet state absorption of the anthracene core. In order to observe the weak bridge state signal, the TA spectra of CdSe NC-PyP4PAn were measured at high 510 nm excitation energy density (1200 μJ/cm^2) using a sample that is saturated with transmitter ligands (4.06 μM CdSe NCs and 0.182 M PyP4PAn, excessive transmitter loading compared to steady-state upconversion measurements). The TA spectra (Figure 4a) are dominated by the CdSe exciton features although additional spectral features of PyP4PAn can also be observed. To better observe the PyP4PAn spectral features, the CdSe signals are removed by subtracting the TA spectra of CdSe /PyP4PAn by the normalized TA spectra of pristine CdSe NCs. The latter has been normalized to the same amplitude at the main exciton bleach peak (~500 nm) as the former at each delay time. The subtracted spectra (Figure 4b) show clearly the GSB (~ 425 nm) and singlet ESA (~ 600 nm) of PyP4PAn at early delay times (<10 ns), and PyP4PAn triplet ESA (~425 nm) at long delay times (~ 1μs). These species are assigned based on the TA spectra of pristine PyP4PAn (Figure S5) that were measured with 440 nm excitation, which directly excites

the singlet excited state of anthracene core (An). Although the PyP4PAn singlet state shown in Figure 4a&b cannot be generated by one photon absorption at 510 nm, it can be generated by multi-photon absorption under the high excitation fluence used in this study.

The subtracted TA spectral also shows a broad peak at ~800 nm at intermediate delay times that is attributed to the bridge triplet state, located on the 4 phenylene units in the conjugated bridge of the PyP4PAn transmitter ligand. The peak position agrees well with low temperature measurements of the tetra-*p*-phenyl triplet state by De Cola.[27, 38] This species is absent in the TA spectra of pristine CdSe NCs and pristine PyP4PAn (Figure S5e), which is more clearly seen in the comparison of these spectra in Figure 4c. This result shows that the bridge triplet state cannot be generated by the excitation of anthracene singlet state. In pristine PyP4PAn, anthracene triplet state can be generated from singlet state via intersystem crossing with a time constant of ~5 ns (Figure S8a, Table S1). In CdSe/PyP4PAn, most of anthracene triplet is formed on a much slower time scale (~200 ns). The growth kinetics of anthracene triplet contains a minor component (~ 5%) that is formed on the ns time scale, suggesting that the direct multiphoton excitation of anthracene singlet state plays a minor role in the formation of triplets. The comparison of the kinetics of the bridge triplet decay (probed at 813 nm) and anthracene triplet growth (probe at 443 nm) in Figure S8b shows that these kinetics are the same, suggesting that bridge triplet is an intermediate in TET from the CdSe NC donor to anthracene acceptor. The transfer rate can be estimated to be 2 us^{-1} from Figure S8b, ~10 times faster than the value in Table 1. This can be explained by the significantly higher PyP4PAn ligand concentration (180 mM compared to 5 mM). The measured triplet energy transfer rate constant agrees with our previous studies on similar system, such as CdSe-ACA and CdSe-T6.[51, 54] This triplet transfer involves a real intermediate localized on the bridge, and is likely controlled by low-frequency vibrational modes in the

tetraphenyl linker[55], or by coupling to nuclear motions of the toluene solvent. Such long distance hopping mediated energy transfer has been shown to be more efficient than coherent superexchange at long distances[56-57]. The results here mirror that observed for charge transfer[58], and for triplet transfer in organics[24, 59], and in d^6 metal diamine donor-acceptor complexes bridged by phenylene units[26-27, 38]. For the $Ru(bpy)_3^{2+}$ (bpy = 2,2'-bipyridine) donor and $Os(bpy)_3^{2+}$ acceptor pair[26], phenylene bridges posed an energetically insurmountable tunneling barrier with an attenuation factor of 0.50 $Å^{-1}$ (similar to the first three ligands here where $\beta = 0.72$ $Å^{-1}$); but for the $Ir(bpy)_3^{2+}$ donor and $Ru(bpy)_3^{2+}$ acceptor couple, a weak distance dependence with of β=0.07 $Å^{-1}$ was attributed to the fact that transfer to the bridge triplet states was exergonic[27].

In conclusion, a systematic study of triplet exciton transfer pathways is enabled by a series of carefully designed transmitter ligands with increasing phenylene bridge units. The upconversion quantum efficiency first decreases exponentially with the increasing distance between the CdSe NC sensitizer and transmitter from zero to two phenylene units (1.4 nm), then remains unchanged with two, three and four units. This result suggests a change in the triplet exciton transfer pathway from a tunneling to hopping mechanism. The hopping mechanism is likely enabled by the gradually lowered triplet state energy of an increased number of phenylene units with a bridge triplet state in resonance with the CdSe donor and anthracene acceptor triplet energy levels. The TA spectroscopy provides a direct observation of triplet excited state on the transmitter and on the bridge. The small donor-bridge gap here of 0.1 eV has been shown to be undesirable for long range energy transfer in organic D-B-A systems[60]. This study suggests that energy transfer will be more efficient with a larger driving force between the donor and bridge, easily achieved by increasing the conjugation length of the bridge, using oligophenylene vinylenes, for example. This work

provides a guide to design hybrid NC-molecule system for efficient and long-range exciton transport for artificial photosynthesis.

Supporting Information

Experimental methods, synthesis, and data fitting procedures are outlined in the Supporting Information. This material is available free of charge at http://pubs.acs.org.

Author Information

Corresponding Author:

tlian@emory.edu.

mltang@ucr.edu

Acknowledgement

MLT acknowledges Air Force Office of Scientific Research (AFOSR) Award FA9550-19-1-0092 for equipment and DOE DE-SC0018969 for salary support. TL acknowledges the financial support by the U.S. Department of Energy, Office of Science, Office of Basic Energy Sciences, Solar Photochemistry Program under Award Number (DE-FG02-12ER16347 and DE-SC0008798). VG acknowledges financial support from Sixten Gemzéus Stiftelse.

References

1. Winkler, J. R.; Gray, H. B., Long-Range Electron Tunneling. *J. Am. Chem. Soc.* **2014,** *136* (8), 2930-2939.
2. Renger, T.; Marcus, R. A., Variable-Range Hopping Electron Transfer through Disordered Bridge States: Application to DNA. *J. Phys. Chem. A* **2003,** *107* (41), 8404-8419.
3. Newton, M. D.; Smalley, J. F., Interfacial bridge-mediated electron transfer: mechanistic analysis based on electrochemical kinetics and theoretical modelling. *Phys. Chem. Chem. Phys.* **2007,** *9* (5), 555-572.

4. Winkler, J. R.; Nocera, D. G.; Yocom, K. M.; Bordignon, E.; Gray, H. B., Electron-transfer kinetics of pentaammineruthenium(III)(histidine-33)-ferricytochrome c. Measurement of the rate of intramolecular electron transfer between redox centers separated by 15.ANG. in a protein. *J. Am. Chem. Soc.* **1982,** *104* (21), 5798-5800.
5. Parson, W. W., Long live electronic coherence! *Science* **2007,** *316* (5830), 1438-1439.
6. Wenger, O. S., Photoinduced electron and energy transfer in phenylene oligomers. *Chem. Soc. Rev.* **2011,** *40* (7), 3538-3550.
7. Skourtis, S. S.; Waldeck, D. H.; Beratan, D. N., Fluctuations in Biological and Bioinspired Electron-Transfer Reactions. *Annu. Rev. Phys. Chem.* **2010,** *61* (1), 461-485.
8. Page, C. C.; Moser, C. C.; Chen, X.; Dutton, P. L., Natural engineering principles of electron tunnelling in biological oxidation–reduction. *Nature* **1999,** *402* (6757), 47-52.
9. Winkler, J. R.; Gray, H. B., Electron Flow through Metalloproteins. *Chemical Reviews* **2014,** *114* (7), 3369-3380.
10. Coropceanu, V.; Cornil, J.; da Silva, D. A.; Olivier, Y.; Silbey, R.; Bredas, J. L., Charge transport in organic semiconductors. *Chemical Reviews* **2007,** *107* (4), 926-952.
11. Solomon, G. C.; Bergfield, J. P.; Stafford, C. A.; Ratner, M. A., When "small" terms matter: Coupled interference features in the transport properties of cross-conjugated molecules. *Beilstein J. Nanotechnol.* **2011,** *2*, 862-871.
12. Wohlthat, S.; Solomon, G. C.; Hush, N. S.; Reimers, J. R., Interference-induced electron- and hole-conduction asymmetry. *Theor. Chem. Acc.* **2011,** *130* (4-6), 815-828.
13. Alivisatos, A. P., Semiconductor Clusters, Nanocrystals, and Quantum Dots. *Science* **1996,** *271* (5251), 933-937.
14. Colvin, V. L.; Schlamp, M. C.; Alivisatos, A. P., Light-emitting diodes made from cadmium selenide nanocrystals and a semiconducting polymer. *Nature* **1994,** *370* (6488), 354-357.
15. Talapin, D. V.; Lee, J.-S.; Kovalenko, M. V.; Shevchenko, E. V., Prospects of Colloidal Nanocrystals for Electronic and Optoelectronic Applications. *Chem. Rev.* **2010,** *110* (1), 389-458.
16. Carey, G. H.; Abdelhady, A. L.; Ning, Z.; Thon, S. M.; Bakr, O. M.; Sargent, E. H., Colloidal Quantum Dot Solar Cells. *Chemical Reviews* **2015,** *115* (23), 12732-12763.
17. Konstantatos, G.; Howard, I.; Fischer, A.; Hoogland, S.; Clifford, J.; Klem, E.; Levina, L.; Sargent, E. H., Ultrasensitive solution-cast quantum dot photodetectors. *Nature* **2006,** *442* (7099), 180-183.
18. Dai, X.; Zhang, Z.; Jin, Y.; Niu, Y.; Cao, H.; Liang, X.; Chen, L.; Wang, J.; Peng, X., Solution-processed, high-performance light-emitting diodes based on quantum dots. *Nature* **2014,** *515* (7525), 96-99.
19. Zhu, H.; Yang, Y.; Wu, K.; Lian, T., Charge Transfer Dynamics from Photoexcited Semiconductor Quantum Dots. *Annu. Rev. Phys. Chem.* **2016,** *67* (1), 259-281.
20. Zhu, H.; Lian, T., Wavefunction engineering in quantum confined semiconductor nanoheterostructures for efficient charge separation and solar energy conversion. *Energy Environ. Sci.* **2012,** *5* (11), 9406-9418.
21. Najafov, H.; Lee, B.; Zhou, Q.; Feldman, L. C.; Podzorov, V., Observation of long-range exciton diffusion in highly ordered organic semiconductors. *Nat. Mater.* **2010,** *9* (11), 938-943.
22. Irkhin, P.; Biaggio, I., Direct Imaging of Anisotropic Exciton Diffusion and Triplet Diffusion Length in Rubrene Single Crystals. *Phys. Rev. Lett.* **2011,** *107* (1), 017402.
23. Peumans, P.; Yakimov, A.; Forrest, S. R., Small molecular weight organic thin-film photodetectors and solar cells. *J. Appl. Phys.* **2003,** *93* (7), 3693-3723.

24. Vura-Weis, J.; Abdelwahed, S. H.; Shukla, R.; Rathore, R.; Ratner, M. A.; Wasielewski, M. R., Crossover from Single-Step Tunneling to Multistep Hopping for Molecular Triplet Energy Transfer. *Science* **2010,** *328* (5985), 1547-1550.
25. Lafolet, F.; Welter, S.; Popović, Z.; Cola, L. D., Iridium complexes containing p-phenylene units. The influence of the conjugation on the excited state properties. *J. Mater. Chem.* **2005,** *15* (27-28), 2820-2828.
26. Welter, S.; Salluce, N.; Belser, P.; Groeneveld, M.; De Cola, L., Photoinduced electronic energy transfer in modular, conjugated, dinuclear Ru(II)/Os(II) complexes. *Coordination Chemistry Reviews* **2005,** *249* (13), 1360-1371.
27. Welter, S.; Lafolet, F.; Cecchetto, E.; Vergeer, F.; De Cola, L., Energy Transfer by a Hopping Mechanism in Dinuclear IrIII/RuII Complexes: A Molecular Wire? *ChemPhysChem* **2005,** *6* (11), 2417-2427.
28. Li, X.; Huang, Z.; Zavala, R.; Tang, M. L., Distance-Dependent Triplet Energy Transfer between CdSe Nanocrystals and Surface Bound Anthracene. *The Journal of Physical Chemistry Letters* **2016,** *7* (11), 1955-1959.
29. Ho Choi, S.; Kim, B.; Frisbie, C. D., Electrical Resistance of Long Conjugated Molecular Wires. *Science* **2008,** *320* (5882), 1482-1486.
30. Huang, Z.; Li, X.; Yip, B. D.; Rubalcava, J. M.; Bardeen, C. J.; Tang, M. L., Nanocrystal Size and Quantum Yield in the Upconversion of Green to Violet Light with CdSe and Anthracene Derivatives. *Chemistry of Materials* **2015,** *27* (21), 7503-7507.
31. Mahboub, M.; Maghsoudiganjeh, H.; Pham, A. M.; Huang, Z.; Tang, M. L., Triplet Energy Transfer from PbS(Se) Nanocrystals to Rubrene: the Relationship between the Upconversion Quantum Yield and Size. *Adv. Funct. Mater.* **2016,** *26* (33), 6091-6097.
32. Huang, Z.; Li, X.; Mahboub, M.; Hanson, K. M.; Nichols, V. M.; Le, H.; Tang, M. L.; Bardeen, C. J., Hybrid molecule–nanocrystal photon upconversion across the visible and near-infrared. *Nano Lett.* **2015,** *15* (8), 5552-5557.
33. Morris, J. V.; Mahaney, M. A.; Huber, J. R., Fluorescence quantum yield determinations. 9, 10-Diphenylanthracene as a reference standard in different solvents. *J. Phys. Chem.* **1976,** *80* (9), 969-974.
34. Gray, V.; Dzebo, D.; Lundin, A.; Alborzpour, J.; Abrahamsson, M.; Albinsson, B.; Moth-Poulsen, K., Photophysical characterization of the 9,10-disubstituted anthracene chromophore and its applications in triplet–triplet annihilation photon upconversion. *J. Mater. Chem. C* **2015,** *3* (42), 11111-11121.
35. Murov, S. L.; Carmichael, I.; Hug, G. L., *Handbook of photochemistry*. CRC Press: 1993.
36. Japar, S.; Ramsay, D. A., Triplet-singlet absorption in pyridine. *J. Chem. Phys.* **1973,** *58* (12), 5832-5833.
37. Berlmann, I. B., *Handbook of Fluorescence Spectra of Aromatic Compounds*. Academic Press: London, 1965.
38. Lafolet, F.; Welter, S.; Popovic, Z.; De Cola, L., Iridium complexes containing p-phenylene units. The influence of the conjugation on the excited state properties. *Journal of Materials Chemistry* **2005,** *15* (27-28), 2820-2828.
39. Nienhaus, L.; Wu, M.; Geva, N.; Shepherd, J. J.; Wilson, M. W. B.; Bulović, V.; Van Voorhis, T.; Baldo, M. A.; Bawendi, M. G., Speed Limit for Triplet-Exciton Transfer in Solid-State PbS Nanocrystal-Sensitized Photon Upconversion. *ACS Nano* **2017,** *11* (8), 7848-7857.

40. Weiss, E. A.; Ahrens, M. J.; Sinks, L. E.; Gusev, A. V.; Ratner, M. A.; Wasielewski, M. R., Making a Molecular Wire: Charge and Spin Transport through para-Phenylene Oligomers. *J. Am. Chem. Soc.* **2004,** *126* (17), 5577-5584.
41. Weiss, E. A.; Tauber, M. J.; Kelley, R. F.; Ahrens, M. J.; Ratner, M. A.; Wasielewski, M. R., Conformationally Gated Switching between Superexchange and Hopping within Oligo-p-phenylene-Based Molecular Wires. *J. Am. Chem. Soc.* **2005,** *127* (33), 11842-11850.
42. Gray, V.; Dreos, A.; Erhart, P.; Albinsson, B.; Moth-Poulsen, K.; Abrahamsson, M., Loss channels in triplet–triplet annihilation photon upconversion: importance of annihilator singlet and triplet surface shapes. *Phys. Chem. Chem. Phys.* **2017,** *19* (17), 10931-10939.
43. Monguzzi, A.; Tubino, R.; Hoseinkhani, S.; Campione, M.; Meinardi, F., Low power, non-coherent sensitized photon up-conversion: modelling and perspectives. *Physical Chemistry Chemical Physics* **2012,** *14* (13), 4322-4332.
44. Dexter, D. L., A Theory of Sensitized Luminescence in Solids. *J. Chem. Phys.* **1953,** *21* (5), 836-850.
45. You, Z.-Q.; Hsu, C.-P., Theory and calculation for the electronic coupling in excitation energy transfer. *Int. J. Quantum Chem.* **2014,** *114* (2), 102-115.
46. Huang, Z.; Simpson, D. E.; Mahboub, M.; Li, X.; Tang, M. L., Ligand enhanced upconversion of near-infrared photons with nanocrystal light absorbers. *Chem. Sci.* **2016,** *7* (7), 4101-4104.
47. Okumura, K.; Mase, K.; Yanai, N.; Kimizuka, N., Employing Core-Shell Quantum Dots as Triplet Sensitizers for Photon Upconversion. *Chemistry – A European Journal* **2016,** *22* (23), 7721-7726.
48. Closs, G. L.; Johnson, M. D.; Miller, J. R.; Piotrowiak, P., A connection between intramolecular long-range electron, hole, and triplet energy transfers. *J. Am. Chem. Soc.* **1989,** *111* (10), 3751-3753.
49. Closs, G. L.; Piotrowiak, P.; MacInnis, J. M.; Fleming, G. R., Determination of long-distance intramolecular triplet energy-transfer rates. Quantitative comparison with electron transfer. *J. Am. Chem. Soc.* **1988,** *110* (8), 2652-2653.
50. Walther, M. E.; Grilj, J.; Hanss, D.; Vauthey, E.; Wenger, O. S., Photoinduced Processes in Fluorene-Bridged Rhenium-Phenothiazine Dyads - Comparison of Electron Transfer Across Fluorene, Phenylene, and Xylene Bridges. *Eur. J. Inorg. Chem.* **2010,** (30), 4843-4850.
51. Jin, T.; Lian, T., Trap state mediated triplet energy transfer from CdSe quantum dots to molecular acceptors. *The Journal of Chemical Physics* **2020,** *153* (7), 074703.
52. Schmidt, T. W.; Castellano, F. N., Photochemical upconversion: the primacy of kinetics. *The journal of physical chemistry letters* **2014,** *5* (22), 4062-4072.
53. Xu, Z.; Huang, Z.; Li, C.; Huang, T.; Evangelista, F. A.; Tang, M. L.; Lian, T., Tuning the Quantum Dot (QD)/Mediator Interface for Optimal Efficiency of QD-Sensitized Near-Infrared-to-Visible Photon Upconversion Systems. *ACS Applied Materials & Interfaces* **2020,** *12* (32), 36558-36567.
54. Xu, Z.; Jin, T.; Huang, Y.; Mulla, K.; Evangelista, F. A.; Egap, E.; Lian, T., Direct triplet sensitization of oligothiophene by quantum dots. *Chemical Science* **2019,** *10* (24), 6120-6124.
55. Davis, W. B.; Ratner, M. A.; Wasielewski, M. R., Conformational gating of long distance electron transfer through wire-like bridges in donor-bridge-acceptor molecules. *Journal of the American Chemical Society* **2001,** *123* (32), 7877-7886.
56. Davis, W. B.; Svec, W. A.; Ratner, M. A.; Wasielewski, M. R., Molecular-wire behaviour in p-phenylenevinylene oligomers. *Nature* **1998,** *396* (6706), 60-63.

57. Davis, W. B.; Wasielewski, M. R.; Ratner, M. A.; Mujica, V.; Nitzan, A., Electron transfer rates in bridged molecular systems: A phenomenological approach to relaxation. *J. Phys. Chem. A* **1997,** *101* (35), 6158-6164.
58. Scott, A. M.; Miura, T.; Ricks, A. B.; Dance, Z. E. X.; Giacobbe, E. M.; Colvin, M. T.; Wasielewski, M. R., Spin-Selective Charge Transport Pathways through p-Oligophenylene-Linked Donor-Bridge-Acceptor Molecules. *Journal of the American Chemical Society* **2009,** *131* (48), 17655-17666.
59. Colvin, M. T.; Ricks, A. B.; Wasielewski, M. R., Role of Bridge Energetics on the Preference for Hole or Electron Transfer Leading to Charge Recombination in Donor-Bridge-Acceptor Molecules. *J. Phys. Chem. A* **2012,** *116* (9), 2184-2191.
60. Davis, W. B.; Ratner, M. A.; Wasielewski, M. R., Dependence of electron transfer dynamics in wire-like bridge molecules on donor-bridge energetics and electronic interactions. *Chem. Phys.* **2002,** *281* (2-3), 333-346.

For Table of Contents Only